Space charge and its role in electric breakdown of solid insulation

George Chen, Churui Zhou
The Tony Davies High Voltage Laboratory
University of Southampton
Southampton, United Kingdom
gc@ecs.soton.ac.uk

Shengtao Li and Lisheng Zhong
State Key Laboratory of Electrical Insulation for Power Equipment
Xian Jiaotong University
Xian, China

***Abstract*—The presence of space charge in solid dielectric materials can lead to electric field distortion and affect the electrical performance. Local electric field enhancement in the solid dielectric materials may greatly contribute to the early aging and even electric breakdown. The above effect has been highlighted in many research papers under HVDC conditions and space charge has been considered as the key to understand many observed phenomena under high electric fields. On the other hand, the influence of space charge in the solid dielectric materials under HVAC conditions has not been fully investigated. In this paper, the effect of space charge on DC breakdown strength of polymeric material has been presented and the thickness-dependent breakdown strength explained using a bipolar charge injection/transport model. More importantly, the model has been extended to AC conditions. Simulations based the model shows the charge dynamics and different features when compared with the DC condition. It can be shown that the breakdown under AC condition is different from that under DC condition. Due to the different charge dynamics the highest electric field is likely to occur in the region close to the surface of the dielectric material under AC condition while in the bulk under DC condition. Consequently, the breakdown strength of a polymeric material under AC condition is lower than that under DC condition. The same model can also be used to explore the effect of frequency and voltage rise rate on the breakdown strength of the polymeric materials. The simulation results show qualitatively agreement with the observed breakdown results.**

Keywords— ***AC electric breakdown; Space charge; Bipolar charge transport; Low density polyethylene (LDPE)***

I. INTRODUCTION

Space charge dynamics within insulation are believed to affect numerical electrical performances of materials. Breakdown strength is a key factor to evaluate dielectrics property under high voltage stresses. Numerous work has been done to understand the relationship between the space charge accumulation and the breakdown phenomenon under DC conditions. [1-3] In 2005, Matsui [2] published a paper, which detected and analysed the space charge behaviour before and right after electrical breakdown under HVDC. From his results, it is clear that space charge contributes greatly to the fields distortion within the insulating materials, and breakdown happens instantly after local electrical fields reach a certain value. Based on that an assumption can be made, for each insulating material, an intrinsic breakdown strength exits, and whenever the local electric field within the material reaches that value, breakdown of the overall material will be triggered. This assumption has been adopted to establish a numerical model analysing breakdown phenomena under dc conditions in 2012 by Chen [3]. The simulated results obtained by the model confirm some general observation in breakdown testing, e.g. apparent strength decreases with increasing sample thickness. [4] And the model has strong experimental evidences in charge formation and transportation in dielectrics under HVDC. Currently, breakdown testing is proceeded under both AC and DC conditions, and normally the results obtained under AC are much lower than those under DC for the same material. Therefore, if the intrinsic strength assumption is accurate, it should be able to explain this gap between the apparent breakdown strengths of the same material obtained under DC and AC conditions.

In this paper, the model in [3] is modified to fit analysing breakdown strengths under more general kinds of applied fields. The modification is strongly based on the measured charge profiles under HVAC/DC conditions. Factors, such as sample thickness, applied fields frequency and testing voltage ramping rate, which affect the apparent dielectric strength are analysed and discussed based on the simulated results.

II. NUMERICAL SIMULATION MODEL

The simulation of the breakdown process is based on the bipolar charge transport theory to analyse charge dynamics inside the insulation. Numerous works were based on bipolar charge theory, commendably analysing the charge dynamics under HVDC, and a group of parameter settings were obtained to tune the calculated results consistent with the measured ones. [5-7] In this work, charge dynamics under HVAC and the more general situation are planned to be investigated. Thus, the parameter setting is modified in this work, and a power's law is adopted to describe the relationship between the mobility of charge carriers and the field's strength. The modification of the parameters has consulted parameter settings in [8], and considered the practical space charge results under HVAC/DC. Besides, ramping applied voltage is used in calculation of the breakdown strength, in order to simulate a real testing situation. An intrinsic breakdown strength is settled. Whenever the maximum electric field within the material reaches the value, breakdown is assumed to have occurred. The current applied voltage is divided by the sample thickness to get the apparent breakdown strength. The specifics of the simulation are discussed in the following sessions.

A. Bipolar charge transport model

Two categories of charges carriers (Electrons and holes) are involved in the bipolar charge transport theory. They both contribute to the injection, transport, and recombination processes within the insulation, and own their unique characteristics. In the work, electrical injection is regarded as the only sources of charges and Schottky mechanism, (1), is used to estimate the process.

$$J_{in} = AT^2 \exp\left(\frac{-ew_{barrier}}{kT}\right)\exp\left(\frac{e}{kT}\sqrt{\frac{eE}{4\pi\varepsilon}}\right) \quad (1)$$

where J_{in} is the injection current density at the electrodes; E is the electric field at the electrodes; A is the Richardson constant; T is the temperature; e is the elementary electronic charge; k is the Boltzmann constant; $w_{barrier}$ is the injection barrier height for charge carriers (specific values for holes and electrons are different); and ε is the permittivity of the dielectrics.

The effects of charge extracting away from the electrodes are analysed using (2) as below:

$$J_{ext} = \mu n E \quad (2)$$

where J_{ext} is the flux of charge carriers, μ is the mobility of charge carriers; and n is the density of mobile charge carriers at the electrodes, and E is the electric field at the electrodes

Charge transport process is described using the mobility of charge carriers. And the mobility has a power's law relationship with electric fields, as shown below. [8,9]

$$J = \mu n E \quad (3)$$

$$\mu = \mu_0 E^{m-1} \quad (4)$$

where J is the conduction current density; μ is the mobility of charge carriers and it is field dependent; μ_0 is the mobility under low electric fields (specific values for holes and electrons are different); m is the power index; n is the density of mobile charge carriers; and E is the local electric field.

During charge transportation, the charge carriers can be captured by some localised defects (traps). And in this paper, traps are ideally divided into two kinds-deep/shallow traps. It is assumed that charges in shallow traps are able to detrap, while those in deep traps are unable to become mobile again. No extraction barrier is considered in this work aiming to simplify the computing procedure. Furthermore, we assume positive and negative charges are prone to recombine with each other. In consideration of all these, the charge transportation in dielectrics is described using three basic equations, (5) to (7).

Poisson's equation:

$$\frac{\partial E(x,t)}{\partial x} = \frac{\rho(x,t)}{\varepsilon} \quad (5)$$

Transport equation:

$$j(x,t) = \mu n(x,t) E(x,t) \quad (6)$$

Continuity equation:

$$\frac{\partial n(x,t)}{\partial t} + \frac{\partial j(x,t)}{\partial x} = s \quad (7)$$

where j is the current density, x is the spatial coordinate, t is the time, s is the source term, ε is the dielectric permittivity, and ρ is the net charge density.

The source term, s, is affected by the charge trapping and recombination process as illustrated in Fig. 1. S_0, S_1, S_2, and S_3 are the recombination coefficients for different opposite species; B_e and B_h are the electrons/holes trapping coefficients.

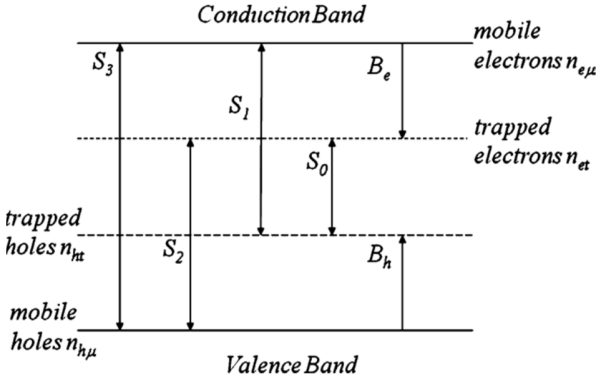

Fig. 1. Illustration of trapping and recombination of bipolar charges.

The total current flux $j_t(x,t)$ is combined by the conduction and displacement current densities as shown in (8).

$$j_t(x,t) = j(x,t) + \varepsilon \frac{\partial E(x,t)}{\partial t} \quad (8)$$

The overall process neglects the effects of charge carrier's diffusion. The recombination of opposite species is represented using total recombination rate(T_R), calculated in (9).

$$T_R = S_0 n_{ht} n_{et} + S_1 n_{ht} n_{e\mu} + S_2 n_{et} n_{h\mu} + S_3 n_{h\mu} n_{e\mu} \quad (9)$$

where $n_{e\mu}$ and $n_{h\mu}$ are the density of mobile electrons and holes; n_{et} and n_{ht} are the density of trapped electrons and holes;

B. Space charge measurements under High voltage electric fields

The charge profiles under HVDC and HVAC are measured in order to evaluate the simulation model. In order to detect charge dynamics under HVAC, an improved PEA system proposed in [10] is used. The phase angles of specific charge profiles are determined according to their integrated electric fields results, rather than peak values (at the entry electrode) of the PEA signals used in [10]. This is because a significant amount of charges may present in the region close to the surface of the insulation even under power frequency HVAC fields [11], which will make the charge peaks at the electrodes not proportional to the applied AC voltage.

The measured charge profiles with the applied voltage are used subtraction method proposed in [12] to remove the influence of capacitive charges within the charge distributions. Decay results are also used to evaluate the trapped charge amount. Fig.2 and Fig.3 present the charge dynamics under 50Hz 50kV/mm HVAC, while Fig 4 and 5 show the trend under HVDC with same strength.

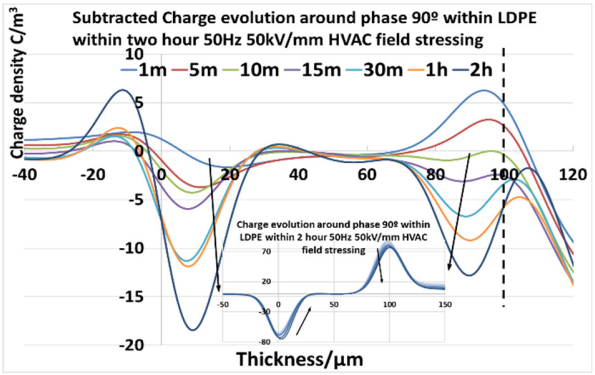

Fig. 2. Charge evolution around applied fields phase 90º after removing the capacitive charge within 2 hours of ac field stressing (50kV/mm)

Combined Fig.2 and 3, it is clear that a large amount of mobile charge exits within the insulation after several hours of HVAC fields aging. The trapped charge amounts are relatively small comparing within mobile ones, and majority of them are negative charges. The mobile charges can only accumulate adjacent the electrodes due to the consistent reversal of the applied fields polarity.

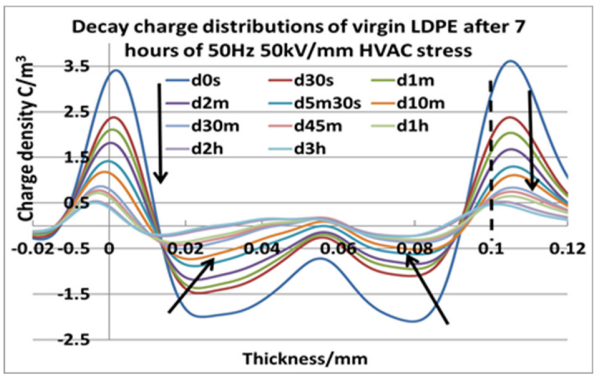

Fig. 3. Decay results of space charge within LDPE after 7 hours of 50Hz 50kV/mm HVAC fields stressing

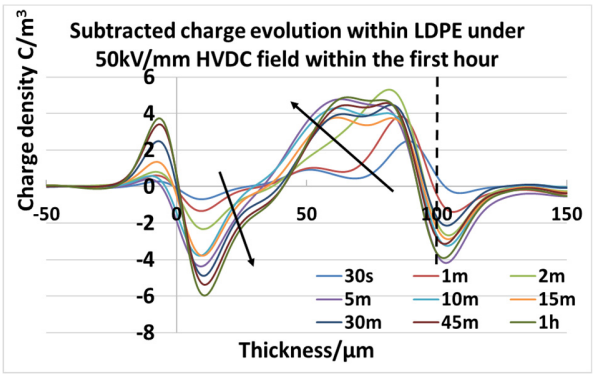

Fig. 4. Charge evolution after removing the capacitive charge within 1 hours of dc field stressing (50kV/mm)

As for charge dynamics under HVDC stresses, it is clear that the accumulated charge amount within insulation is larger than that under HVAC, and both positive and negative charge are able to accumulate and transfer further into the bulking area of the sample. And combined Fig.4 and 5, it is obviously that the accumulated charges under HVDC are mainly trapped charges.

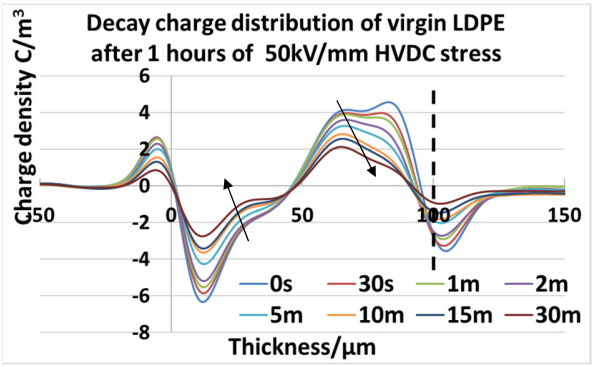

Fig. 5. Decay results of space charge within LDPE after 1 hours of 50kV/mm HVDC fields stressing

C. *Simulation settings and comparison with measured results*

In this work, simulation parameters are selected based on the comparison of the calculated and measured charge profiles under constant strength fields. According to measurements, negative charges dominate the charge dynamics under HVAC. Therefore, lower Schottky injection barrier and high mobility are designed for electrons. Besides, mobile charge amount is much higher trapped charge one under HVAC (Figs.2 and 3). Thus lower trapping coefficients ($<1\times10^{-2}$) are used for both carriers. After many iterations, trial and adjustments, the final adopted parameters are listed in Table I. An example of computed charge dynamics under HVAC and HVDC are presented in Fig.6 and Fig,7.

TABLE I. PARAMETERS FOR CHARGE DYNAMICS SIMULATION OF BREAKDOWN STRENGTH TEST

Parameter	Value	Unit
Barrier height for injection		
W_{ei} *(electrons)*	1.1	eV
W_{hi}*(holes)*	1.12	eV
Low field Mobility μ_{E0}	9×10^{-16}	$m^2V^{-1}s^{-1}$
Low field Mobility μ_{h0}	3×10^{-16}	$m^2V^{-1}s^{-1}$
Power law's index of mobility m	1.165	
Trap density		
N_{0et} *(electrons)*	100	Cm^{-3}
N_{0ht} *(holes)*	100	Cm^{-3}
Trapping coefficients		
B_e *(electrons)*	7×10^{-3}	s^{-1}
B_h *(holes)*	7×10^{-5}	s^{-1}
Recombination coefficients		
S_0 *trapped electron-trapped hole*	4×10^{-3}	$m^3C^{-1}s^{-1}$
S_1 *mobile electron-trapped hole*	4×10^{-3}	$m^3C^{-1}s^{-1}$
S_2 *trapped electron-mobile hole*	4×10^{-3}	$m^3C^{-1}s^{-1}$
S_3 *mobile electron-mobile hole*	0	$m^3C^{-1}s^{-1}$
Temperature T	300	K
Intrinsic breakdown strength	5×10^8	Vm^{-1}

From Fig.6 it is obviously that, negative charges dominate the charge accumulation, and are able to transfer further into the bulk of the insulation. The calculated net charge dynamics are identical to the trapped charge trend presented in Fig.3. Besides the computed mobile charge amounts are much larger than the trapped charge amount, and the majority of the mobile charges,

regardless of polarity, are accumulated adjacent the electrodes. These are also consistent with the observation in the subtracted results (Fig.2). The simulation gives a picture of an ideal case where applied fields phase is zero. Therefore, the obtained mobile electrons and holes amounts are relatively similar. This convinces mobile charge can evolve along with the changing of the applied fields within the surface region of the insulation under high frequency HVAC stresses. (Similar phenomenon presented in Fig.2) Fig.7 presented the simulated charge profiles under HVDC. Although the specific charge amounts have some differences, the positive and negative charges dynamics are similar to those in Fig.4 and 5. Positive and negative charges encounter in the middle area of dielectrics, and the accumulated charge amounts are bigger than those under HVAC. Comprehensively, the adopted model can simulate the basic charge dynamics within insulation under both HVAC and HVDC conditions, and it is reasonable to use it to analyse charge dynamics under ramping voltage mode, and to investigate the breakdown process.

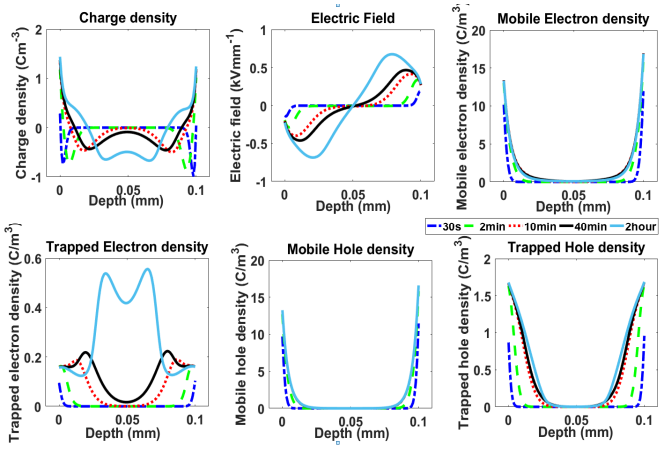

Fig. 6. Simulated charge profiles under 50kV/mm HVAC stress at phase 0

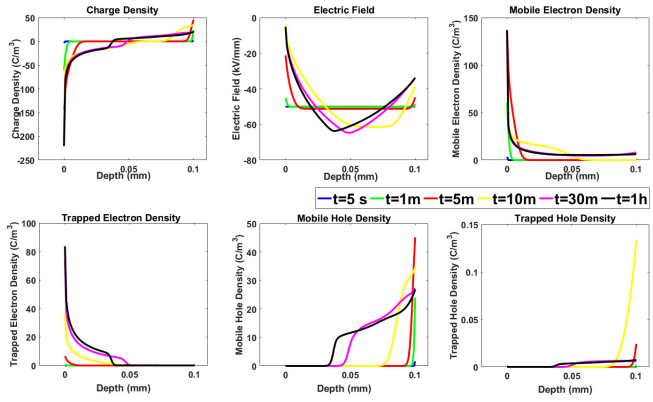

Fig. 7. Simulated charge profiles under 50kV/mm HVDC stress

During the breakdown test, the voltage is applied from the two electrodes to the sample with a fixed ramping rate until the breakdown occurs. The ramping breakdown measurement system typically can test samples up to 0.1 mm thick and the range of ramp rates can vary from 10 to 300 V/s. The typical ramp rate for samples under DC voltage is 100 V/s, whilst 50V/s for sinusoidal AC voltage [13, 14]. Therefore, in the numerical modelling, the external applied voltage is defined as following:

$$V = R \cdot t \cdot \sin(2\pi \cdot f \cdot t) \tag{10}$$

where R is the ramping rate and f is the external voltage frequency. In the simulation process, R and f can be changed according to the analysis requirements.

The simulated material is a low density polyethylene film with a thickness ranging from 50 to 200 μm. From the existing experimental results in [2], it has been observed that the breakdown occurs when the local electric field strength in polyethylene is around 500 kV/mm. Thus in our simulation, the intrinsic breakdown strength is settled to be 500kV/mm. Whenever, the maximum local field reaches that value, the breakdown is considered to have occurred. And the apparent breakdown strength can be deduced using (11).

$$S = \frac{V_B}{D_T} = \frac{R \cdot T_0}{D_T} \tag{11}$$

where S is the apparent breakdown strength; V_B is the applied voltage when breakdown happens: D_T is the testing sample thickness and T_0 is the field stressing time to achieve breakdown.

III. CHARGE DYNAMICS AND THEIR ROLE IN BREAKDOWN REGION OF THE INSULATING MATERIAL

Numerous mechanisms (electronic, avalanche, electromechanical, thermal breakdowns, partial discharges) have been proposed to explain the breakdown process. [15] However, few of them investigated the specific region where breakdown happens. From the charge dynamics presented in the above section (Fig.2-7), it is clear that large amounts of charge accumulate at different regions within the insulation under HVAC and HVDC stresses. Those charges can severely distort the local electric fields within the insulation. Based on our electrical breakdown theory, the place where breakdown occurs should be effected by those charges, and be divergently located under HVAC and HVDC fields. The relationship between this divergence and different AC and DC breakdown strengths of same materials will be figured out in this session.

Fig.8-10 present an example demonstrating the charge distributions and electric fields within material under HVAC and HVDC when breakdown happens. And the marking points are the place where breakdown happens. The simulation condition for this two are the same, except for the applied field's types. From graphs, it is clear that the charge dynamics within insulation under AC and DC ramping stresses are different. Under AC stress, charges can only accumulate adjacent the electrode while under DC, they can transfer into the bulking arear of the material. These divergent charge distributions cause different local fields distortion, which eventually makes the value and the location of the maximum electric fields (where breakdown happens) different. The field distortion adjacent the electrodes is normally more intensive, as less amount of charge and smaller charge transport distance needed to cause the distortion, comparing with distortion in the middle area under same strength. Thus, the maximum electric field of ac condition is more easily and rapidly to reach the breakdown level comparing with under same strength DC stress, which makes the

apparent breakdown strength lower. (160.8kV/mm for 50Hz AC and 421.8kV/mm for DC)

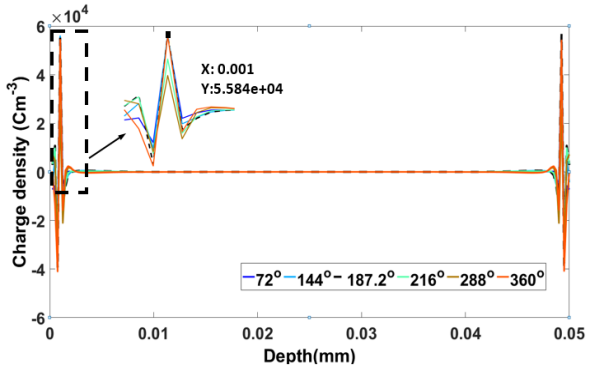

Fig. 8. Charge profiles corresponding to breakdown cycle for 50um LDPE under 50Hz HVAC with a ramping rate of 50V/ s (Apparent breakdown strength: 160.8 kV/mm)

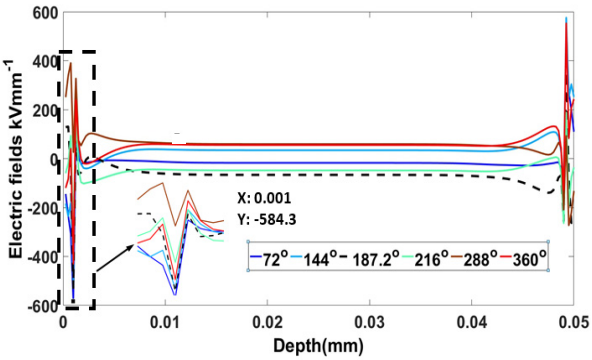

Fig. 9. Electric fields profiles corresponding to breakdown cycle for 50um LDPE under 50Hz HVAC with a ramping rate of 50V/s (Apparent breakdown strength: 160.8 kV/mm)

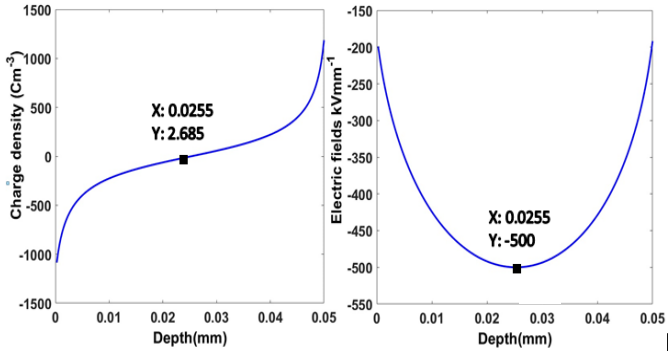

Fig. 10. Charge and electric fields profiles at the breakdown for 50um LDPE under HVDC with a ramping rate of 50V/s (Apparent breakdown strength: 421.8 kV/mm)

Fig 8-10 only involve the cases of charge dynamics and apparent breakdown strength under DC and relatively high frequency AC stresses (50Hz). In order to figure out how charge dynamics cause the apparent breakdown strength changing with frequency, Fig.11 presents the distance of the breakdown region (left ordinate) and apparent breakdown strength (right ordinate) evolving along with frequency adding. It is obviously that breakdown happens more close to the electrodes when applied fields frequency is higher. This indicates charges under higher frequency applied fields are harder to transport into the bulking area of the insulation. And because majority of them accumulate more closely to the electrodes with the adding frequency, the field within the surface region of the material is more severely and rapidly distorted. Therefore, breakdown can be triggered under lower strength when the applied field's frequency is higher.

Breakdown region is the place where the local electric field is most severely distorted. And to some extent, breakdown region can represent where the most intensive charge dynamics happens in the insulation. Besides from Fig,11, it is also clear that the distance of breakdown region towards electrode demonstrates a similar trend as the apparent breakdown strength when ramping rate (R) and thickness(D_T) are fixed. Therefore, in some degree, the distance, D, is proportional to the stressing time to achieve breakdown, T_0, based on (11). This means the breakdown region can, as a factor, indicate how rapidly the breakdown process conducts. ($T_0 \propto D$)

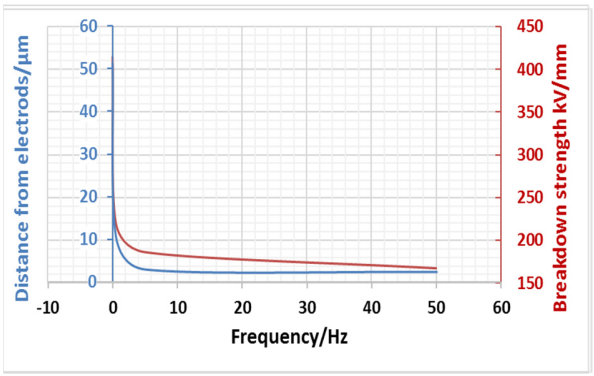

Fig. 11. The distance of breakdown region towards electrodes and breakdown strength of 100 μm samples under various frequency applied fields with ramping rate 100V/s

All these above confirm the assumption that the apparent breakdown strengths of insulating materials are strongly related to the region where breakdown happens. Breakdown happens more rapidly and more closely to the surface of the material when the frequency of applied fields is higher. The more severely unbalanced and distorted electric fields, caused by charge dynamics, is a significant reason leading the lower apparent breakdown strengths of same materials under HVAC comparing with under HVDC. Besides, the investigation of breakdown region can link the specifics charge dynamics with the overall material characteristics, which should be much more concerned in the study of breakdown process.

IV. Relationship between Breakdown Strengths and Testing Sample Thickness

Based on numerous experimental results [4,16-17], the apparent breakdown strength of insulating material demonstrates a decreasing trend along with adding testing sample thickness. An inverse power's law, shown in (12), is generally used to analyse the trend [4], and the principle can apply to various kinds of dielectrics under divergent conditions.

However, this principle is purely empirical and many attempts (defect, percolation and threshold theories) have been tried to explain the phenomenon. Most of them are lack of creditable experimental results and not able to describe dynamics in the material under higher electric fields. [3]

$$E(d) = k \cdot d^{-n} \tag{12}$$

where E is the applied electric field at breakdown, in this paper it is equal to S, and k and n are two constants that are associated with the testing material.

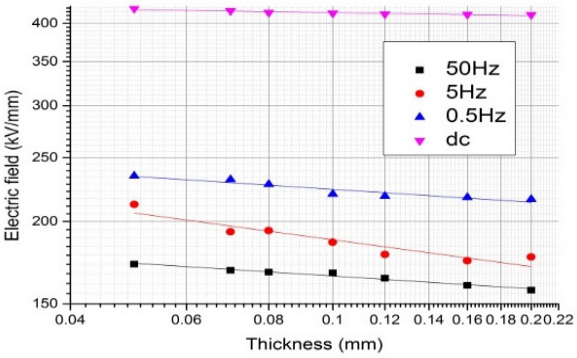

Fig. 12. Breakdown strengths versus sample thickness under different frequencies fields (Fitted index of power law: -0.0645—50Hz, -0.1351—5Hz, -0.0653—0.5Hz, -0.0151—DC)

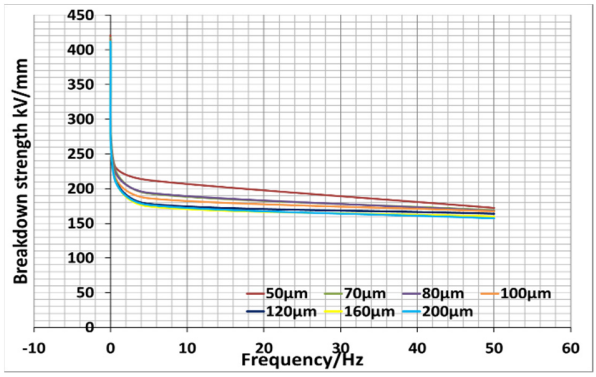

Fig. 13. Breakdown strengths versus frequencies within different thickness sample

In this section, the relationship of the sample thickness and breakdown strengths is analysed and discussed using the simulated results with a range of thickness from 50μm to 200μm under different frequency stresses with a fixed voltage ramping rate of 100V/s. The calculated results are presented in Fig.12 and 13. Fig.12 demonstrates the calculated apparent breakdown strengths of materials decreasing along with the increasing of testing sample thickness. The reduction trend follows the inverse power's law, consistent with the phenomena observed in experiments [4]. From the fitted indexes of the power's law under various applied fields frequencies, it is clear that the breakdown strength changes more severely with the alteration of the thickness under AC stress. But all the fitted power indexes are smaller than normal value, 0.5, observed in measurements. [4] This indicates the apparent breakdown thickness dependent phenomenon is an integral characteristic caused by multiple factors. Charge dynamics under high voltage stress are only part of the reason. Defects, percolation and some other procedure may have also contributed to the trend. Fig.13 presents the results in Fig.12 in another view. In Fig.13, the trend of apparent breakdown strength decreasing within increasing of the applied frequency under all cases is more directly illustrated. And it is easy to distinguish that the apparent breakdown strength presents more significant differences among various thickness samples results, when the applied fields' frequency is within 0.5Hz to 20Hz range. And for all frequency cases, the apparent breakdown strength decreases sharply when the thickness enhancing from 50μm to 100μm. The differences of the strength among sample thickness beyond 100μm are relatively small.

The distance of breakdown region towards electrodes of various thickness testing sample is recorded in Fig.14, in order to directly illustrate how inter charge dynamics cause the apparent breakdown strength changing with thickness. Results under 0.5Hz fields are chosen to discuss, as charge can evolve within a relative large region under this lower frequency AC stresses. From Fig.14, it is clear that the distance D increases, while the distance to thickness ratio, $(\frac{D}{D_T})$, decreases along with thickness adding. The trends in Fig.14 indicates the electric fields distortion, caused by sever charge dynamics in surface region under HVAC, is alleviated along with the testing sample thickness increasing. But this relief is quite limited, as in thicker samples, the localised charges will become more difficult to transport to the other side. Breakdown still happens adjacent to the electrodes (from $(\frac{D}{D_T})$, it is actually closer) within thicker samples under HVAC stresses with relative high frequency (>0.5Hz).

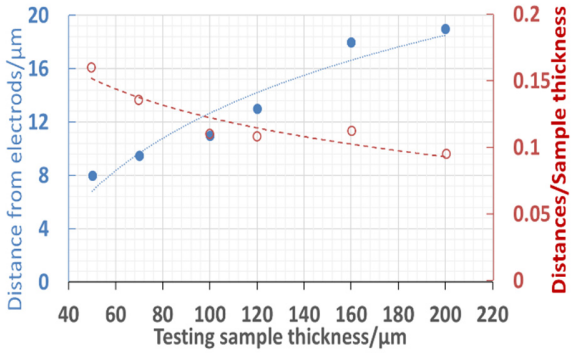

Fig. 14. The distance of breakdown region towards electrodes of various thickness samples under 0.5Hz HVAC fields with ramping rate 100V/s

From analysis of Fig.11, it is clear that the fields stressing time to breakdown $T_0 \propto D$. And based on (11), it can be deduced that apparent breakdown strength, $S \propto (\frac{D}{D_T})$, when ramping rate, R, is fixed. Because $(\frac{D}{D_T})$ decreases along with thickness adding, the apparent breakdown strength reducing accordingly. Besides, the fitted trend line of $(\frac{D}{D_T})$ vs. D_T (thickness) seems to have decreasing level of changing, which indicates the extent of $(\frac{D}{D_T})$ changing reducing along with thickness adding. And that's why limited change of breakdown strength can be found for all

frequency cases when the testing sample thickness is bigger than 100 μm. Furthermore, when applied fields frequency increases, D reduces, but the extent of the changing is also decreasing. (Fig.11) And that explains the significant differences observed among results under applied voltage with frequency lower than 20Hz in Fig.13.

In summary, the computed apparent breakdown strength shows a similar relationship with the testing sample thickness comparing with observation in practice. This confirm the charge dynamics within the insulation is a significant reason causing the apparent breakdown strength affected by thickness. The apparent breakdown strength can have an enormous gap between the intrinsic breakdown, especially for thicker sample under higher frequency applied fields. Breakdown region can be recorded as a factor containing information of charge dynamics and electric fields distortion, to explain the relationship between apparent breakdown strength and testing sample thickness. The simulation model and explanation in this paper are quite preliminary design, and based on many assumption aiming to simplify the situation. In reality, the trend of apparent breakdown strength decreasing with testing sample adding, should be caused by numerous reasons, and the charge dynamic with the insulation is only part of them. But based on the results shown in this session, bipolar charge theory demonstrates a promising possibility to simulate and investigate the dynamics within breakdown process.

V. Relationship between Breakdown Strength and Voltage Ramping Rate

It has been reported that the ramping rate of the applied voltage can influence the measured apparent breakdown strength of the material. Different ramping rates have been used to measure the breakdown strength in various publications [4,13-14]. In order to compare the apparent breakdown strength obtained by the measurements with different ramping rates, the effect of the ramping rate on breakdown strength is analysed and discussed using the proposed model.

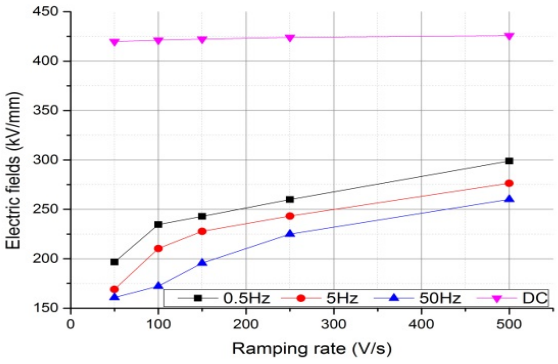

Fig. 15. Breakdown strengths under different outer fields' ramping rate and frequencies

Fig 15 presents the computed apparent breakdown strength under both HVAC and HVDC conditions. For both conditions, the material breakdown strength increases along with the ramping rate rising. A similar trend for the apparent breakdown strength has been observed experimentally. [18] Rapid increase of the apparent breakdown strength happens from the ramping rate adding from 50V/s to 250V/s. However, it seems the ramping rate has severer influence on apparent strengths under AC conditions. From 50V/s to 500V/s, a change of more than 100kV/mm has been observed. This may be account for the differences in testing breakdown strength for materials under AC conditions presented in literature. Even for the same testing system and testing environment, the influence caused by the various ramping rates should also be taken into consideration for comparing breakdown strengths of material under HVAC electric fields.

The distance of breakdown region towards electrodes (D) under different ramping rates (R) is recorded and analysed in Fig.16. An initial approach is proceeded here to explain how charge dynamics can cause the apparent breakdown strength increasing along with ramping rate adding. From Fig.16, it is clear that the distance D decreases, while the product of the distance and ramping rate, $(D \cdot R)$, increasing along with thickness adding. This indicates severe charge dynamics within insulation happens more closely towards electrodes, under higher ramping rate stresses. But the influences of these dynamics on the local fields distribution are weaken along with ramping rate increasing. This is because under higher ramping rate fields, it takes shorter time to achieve the same applied fields strength and the charge formation and transport require certain time to cause severe fields distortion.

Based on (11) as well as $T_0 \propto D$, S (apparent breakdown strength)$\propto (D \cdot R)$, when thickness, D_T. is fixed,. Because $(D \cdot R)$ increases along with thickness adding, the apparent breakdown strength enhances accordingly.

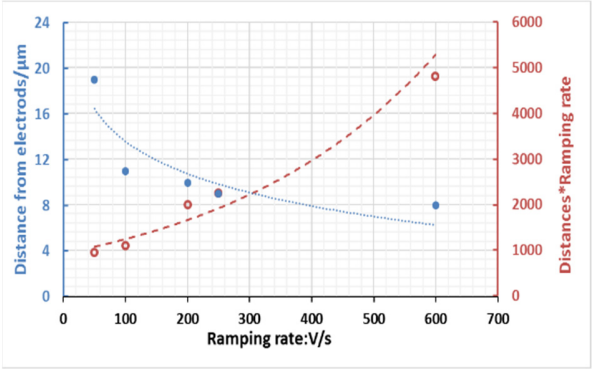

Fig. 16. The distance of breakdown region towards electrodes of 100 μm samples under 0.5Hz HVAC fields with different ramping rates

In conclusion, the apparent breakdown strength increases along with applied field's ramping rate adding. In evaluation of materials' breakdown strength, the ramping rate's effects should be taken into account. Currently, there is no general agreed trend illustrating how apparent breakdown strength adding with the ramping rate raising. The work here presents a possibility to use simulation and analysis of charge dynamics within insulation during the breakdown process deducing and explaining the relationship. But large amounts of experimental work are still needed to convince the trend and explanation.

VI. Conclusion and Future Work

The paper proposed a breakdown process simulation model suitable for analysis for both AC and DC conditions, based on bipolar charge transport theory. The influences of common factors, applied field's frequency, testing sample thickness and applied field's ramping rate, have been investigated and explained based on the model. The obtained charging trends of apparent breakdown strength are consistent with general observation in breakdown strength measurements. This confirmed the possibility to use charge dynamics to explain and deduce material overall characteristics, like apparent breakdown strengths. It has also been found that the apparent breakdown strength is strongly related to the place where breakdown happens. The different breakdown happen region caused by divergent charge dynamics is a significant reason leading the apparent breakdown strength of same material under AC and DC conditions different. Different testing sample thickness as well as applied field ramping rate can also change the breakdown happening region.

In future, the simulation theory will be modified according to the charge measurements under ramping voltage mode, in order to more accurately consider the charge dynamics during the breakdown process. The influences of defect and percolation will be taken into account to define when breakdown happens. It will not ideally like current, assuming breakdown happens wherever the local electric fields reach a certain value, and the testing sample has uniform electric characteristics. The extent of the aging and damaging will also be investigated at different regions of the breakdown tested samples to experimentally confirm that the place where breakdown happens will be different under divergent categories of applied fields.

Acknowledgment

The preferred spelling of the word "acknowledgment" in America is without an "e" after the "g". Avoid the stilted expression "one of us (R. B. G.) thanks ...". Instead, try "R. B. G. thanks...". Put sponsor acknowledgments in the unnumbered footnote on the first page.

References

[1] A. Bradwell, R. Cooper, and B. Varlow, "Conduction in polythene with strong electric fields and the effect of prestressing on the electric strength," in Proceedings of the Institution of Electrical Engineers, 1971, pp. 247-254.

[2] K. Matsui, Y. Tanaka, T. Takada, T. Fukao, K. Fukunaga, T. Maeno, et al., "Space charge behavior in low density polyethylene at pre-breakdown," IEEE Trans. Dielectr. Electr. Insul. , 2005, vol. 12, pp. 406-415.

[3] G. Chen, J. Zhao, S. Li, and L. Zhong, "Origin of thickness dependent dc electrical breakdown in dielectrics," Appl. Phys. Lett. , 2012, vol. 100, p. 222904.

[4] H. Kim and F. Shi, "Thickness dependent dielectric strength of a low-permittivity dielectric film," IEEE Trans. Dielectr. Electr. Insul. , 2012, vol. 8, pp. 248-252.

[5] J. Alison and R. Hill, "A model for bipolar charge transport in insulators," in Conduction and Breakdown in Solid Dielectrics, 1995. ICSD'95., Proceedings of the 1995 IEEE 5th International Conference, 1995, pp. 319-323.

[6] S. Roy, G. Teyssedre, P. Segur, and C. Laurent, "Modelling of space charge, electroluminescence and current in low density polyethylene under DC and AC field," in Electrical Insulation and Dielectric Phenomena, CEIDP Annual Report Conference, 2004, pp. 29-32.

[7] J. Zhao, G. Chen, and P. L. Lewin, "Investigation into the formation of charge packets in polyethylene: Experiment and simulation," J. Appl. Phys., 2012, vol. 112, pp. 034116-034116-6.

[8] J. Zhao, Z. Xu, G. Chen, and P. L. Lewin, "Numeric description of space charge in polyethylene under ac electric fields," J. Appl. Phys., 2010, vol. 108.

[9] T. Sonnonstine and M. M. Perlman, "Surface-potential decay in insulators with field-dependent mobility and injection efficiency," J. Appl. Phys. , 1975, vol. 46, pp. 3975.

[10] J. Zhao, G. Chen, and L. S. Zhong, "Space Charge in Polyethylene under Combined AC and DC Voltages," IEEE Trans. Dielectr. Electr. Insul. , 2014, vol. 21, pp. 1757-1763.

[11] C. Zhou and G. Chen, "Space charge and AC electric breakdown strength in polyethylene," in Electrical Insulation and Dielectric Phenomena (CEIDP), 2015 IEEE Conference, 2015, pp. 106-109.

[12] N. Liu, C. Zhou, G. Chen, and L. Zhong, "Determination of threshold electric field for charge injection in polymeric materials," Appl. Phys. Lett. , 2015, vol. 106, p. 192901.

[13] N. Hussin, J. Zhao, and G. Chen, "The AC breakdown and Space Charge Characteristics of LDPE in the presence of Crosslinking Byproduct," in Electrical Insulating Materials (ISEIM), Proceedings of 2011 International Conference, 2011, pp. 65-68.

[14] M. Nagao, K. Takano, Y. Mizuno, and M. Kosaki, "Intrinsic Ac Breakdown of Low-Density Polyethylene Film above Room-Temperature," Proceedings of the 3rd International Conference on Properties and Applications of Dielectric Materials, 1991, vols 1 and 2, pp. 1165-1168.

[15] V. Zakrevskii, N. Sudar, A. Zaopo, and Y. A. Dubitsky, "Mechanism of electrical degradation and breakdown of insulating polymers, J. Appl. Phys. , 2003, vol. 93, pp. 2135-2139.

[16] B. Epstein and H. Brooks, "The theory of extreme values and its implications in the study of the dielectric strength of paper capacitors," , 1948, J. Appl. Phys. , vol. 19, pp. 544-550.

[17] S. Cygan and J. Laghari, "Dependence of the electric strength on thickness area and volume of polypropylene," IEEE Trans. Dielectr. Electr. Insul. , 1987 , pp. 835-837.

[18] C. Chauvet and C. Laurent, "Weibull statistics in short-term dielectric breakdown of thin polyethylene films," IEEE Trans. Dielectr. Electr. Insul. , 1993 , vol. 28, pp. 18-29.